



Reliable uplink transmissions for NOMA-based Industrial Wireless Networks with guaranteed real-time performance

Chaonong Xu^{a,*,} Jianxiong Wu^a, Chao Li^b

^a Beijing Key Lab of Petroleum Data Mining, China University of Petroleum, Beijing, 102249, China

^b Institute of Computing Technology, China Academy of Sciences, Beijing, 100190, China



ARTICLE INFO

Keywords:

Successive Interference Cancellation
Uplink Scheduling
Power control
Delay guarantee
Reliability

ABSTRACT

Reliability is vital for ultra-reliability low-latency transmission applications in Industrial Wireless Networks (IWNs). The power-domain Non-Orthogonal Multiple Access (NOMA) technology can support multiple parallel transmissions, and has been thought of as one of the most powerful candidate radio access technology for the next-generation IWNs. However, it suffers from low transmission reliability because of the high interferences caused by parallel transmissions in power-domain NOMA. In this paper, given the real-time performance requirements, we consider a single-hop network supporting 2-Successive Interference Cancellation, and study how to maximize the reliabilities of uplink transmissions by the joint user pairing and power allocation. We show that the problem is solvable in polynomial time by an optimal algorithm with complexity of $\mathcal{O}(n \log n)$, where n is the number of users. The performance evaluations reveal that the transmission reliabilities will increase exponentially with the linear degradation of the guaranteed real-time performance.

1. Introduction

Communication reliability and transmission delay are two important performance metrics for applications in Industrial Wireless Networks (IWNs). Therefore, Ultra-Reliability Low-Latency Communications (URLLC) are considered as one of the key technologies for the next-generation IWNs [1]. In many applications in IWNs, low delay guarantee instead of low average delay is rigidly required, since outdated sensory data is of no meaning for some time-sensitive applications, such as the real-time controls in oil well exploiting [2]. Thus, media access technologies with high transmission reliability and the guaranteed real-time performance for uplinks are urgently required in IWNs.

In recent years, the power-domain non-orthogonal multiple access (NOMA) technology is utilized in IWNs [3

In all, BPSK based 2-SIC technology is valuable for URLLC applications in IWNs.

We focus on a typical IWN topology, where multiple users transmit data to a BPSK based 2-SIC sink. The focus of this paper is how to maximize the total uplink transmission reliability of all users, under the premise of the guaranteed real-time performances, by joint user pairing and power allocation [9].

We have proved that for the optimal solution to the problem, the user pairing strategy and the power allocation strategy are independent with each other. Therefore, the joint optimization problem can be converted into a two-stage optimization problem. In other words, we can still find an optimal strategy by a two-steps algorithm framework as follows; first, finding an optimal user pairing strategy, and second, finding an optimal power allocation strategy under the above optimal user pairing strategy.

Our technical contributions are summarized as follows. (1) A reliability model of power-domain NOMA transmission is elaborated. Specifically, the uplink transmission reliability of a BPSK-modulated NOMA system with multiple users and one sink is modeled, and thus a closed-form expression of transmission reliability, which is based on the average bit error rate of multiple users, is presented. (2) It is proved that the original problem can be decomposed into a two-stage optimization problem: namely, a multi-slot user scheduling sub-problem and a single-slot power allocation sub-problem, and the decomposition greatly reduces the complexity of problem solving. (3) For the single-slot power allocation sub-problem, an optimal power allocation strategy is designed. For the multi-slot user scheduling sub-problem, an optimal user grouping algorithm is designed. (4) Based on the theoretic foundation and the algorithms designed, a reliability-optimal algorithm with guaranteed delay is designed with complexity of $O(n \log n / \log n)$.

This remainder of this paper is organized as follows. Section 2 is related works, and Section 3 elaborates the receiving model of signals from 2-SIC, which is the foundation of all theoretical analyses. Section 4 is the theoretic preliminaries of this paper. In Section 4.1, the closed-form BER expression of two parallel users is proposed, which is the base for all lemmas and theorems in this paper. In Section 4.2, there are some theoretic preliminaries based on closed-form BER expression proposed in Section 4.1, and besides, the minimal BER of two users in one time slot is elaborated. The cases of three users in two slots and four users in four slots are deduced in Section 4.3 and Section 4.4, respectively. In Section 4.5, we propose an optimal allocation strategy for two parallel users, which is the base of user scheduling strategy. We start to deal with the reliable uplink transmissions problem in Section 5 as follows; Section 5.1 formulates the problem, and Section 5.2 figures out the independency between the power allocation and the user pairing, and then the optimal algorithm is introduced based on the independency. Section 6 is the performance evaluations, and the last section is the conclusions. The logic structure of this paper is also illustrated in Fig. 1 for clarity, where arrows depict theoretic dependencies. Besides, all notations in the paper are listed in Table 1 for convenience.

2. Related works

S. Loyka and etc. analyzed the reliability of NOMA for Multiple Input Multiple Output (MIMO) system [10], where the reliability was defined as the outage probability of transmissions. It presented a closed-form expression for the probability of error-free transmissions. For the Rayleigh-fading multiple-antenna channels, Shen and etc. presented a reliability model for SIC system with BPSK modulation [11]. Both [10] and [11] are Vertical Bell Labs Layered Space Time (VBLAST) based system. Obviously, it was distinct from that in the power-domain NOMA based system, where there was only one antenna on the receiver. Dinh-Thuan and etc. analyzed the outage probability of energy harvesting NOMA in [12], and Kader and etc. analyzed the outage probability, and outage sum capacity of full-duplex NOMA in [13].

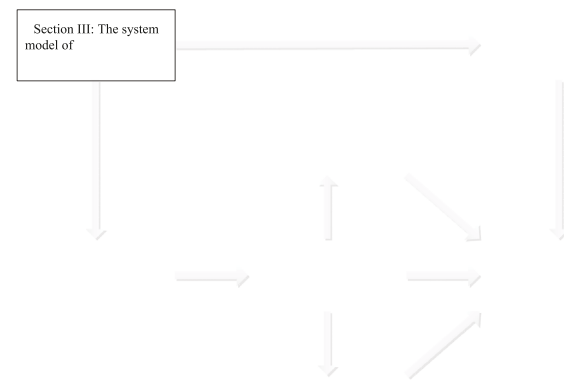


Fig. 1. Logic structure of this paper.

Wang and etc. proposed a more fine-grained reliability model of 2-SIC decoder, where the probability of the partially successful decoding is considered [14]. Based on our reliability model where the case of the partially successful decoding is omitted, we, however, proposed a low-complexity reliability-optimal scheduling strategy. Comparatively, to balance the complexity and the optimality for downlink transmissions, Shi and etc. employed random grouping strategy [15]. In [16], the optimal user pairing strategy was proposed to minimize the aggregate transmitting power, however, the transmission reliability was not taken into considerations. Hina and etc. provided a framework to analyze multi-cell uplink NOMA systems in [17]. In [18], the author formulated a sum-throughput maximization problem and optimized minimum rate requirements of the users. Tasneem and etc. made the exact BER performance analysis for downlink NOMA system over Nakagami-m fading channels in [19]. Ferdi and etc. analyzed the BER performances of downlink and uplink NOMA in the presence of SIC errors over fading channels in [20].

Bin. X and etc. presented closed-form expressions of the outage probability of each user for an uplink 2-user NOMA system [21]. Gyeongrae and etc. derive an exact closed form of the outage probability for each secondary destination in cognitive radio network, considering that the channel coefficients between the primary source and the secondary receiving nodes follow Rayleigh distribution [22]. Worawit and etc. proposed a power allocation scheme based on a deep learning approach for maximizing the sum rate for downlink NOMA system [23]. Aitong and etc. presented an outage performance of NOMA-based unmanned aerial vehicle assisted communication with imperfect SIC [24].

RFID has also enormous applications in enhancing the reliability of IWns. A collaborative decoding method is proposed to overcome the low time-efficiency and the information corruption issue in range query of sensor-augmented RFID systems [25]. In [26], the hash-collision is utilized to support parallel transmissions from multiple RFID and it is obviously helpful for improving reliability of IWns.

3. System models

We consider a network of single-hop, single channel wireless network consisting of N single-antenna User Equipments (UEs) and a single-antenna sink. The sink is equipped with a BPSK-based 2-SIC receiver. A 2-SIC receiver can decode at most two signals in one time.

In the considered network, time is divided into frames, and a frame is divided into multiple time slots. The maximal transmit powers of all users are the same, and the transmit power is continuously adjustable. We only consider perfect interference cancellation, i.e., the residual error is zero, which has been widely adopted [27]. The channel gain

Table 1

Notations.

Y	Received signal at the sink
U_i	User i
G_i	Channel gain of U_i to the sink
P_i	Transmit power of U_i
X_a, X_b	Transmitted symbols by Alice and Bob, $X_a, X_b \in \{1, -1\}$
A_i	Normalized received amplitude of U_i
\hat{A}_i	Maximum received normalized amplitude of U_i
$BE_{A_a; A_b}$	Bit error number when normalized received amplitudes of Alice and Bob are A_a and A_b
$BER_{A_a; A_b}$	Bit error rate when normalized received amplitudes of Alice and Bob are A_a and A_b
$A_{ A_a}$	$\arg \min_{A_b} BER_{A_a; A_b}$ given A_a
$\hat{A}_{b A_a}$	The minimum of $A_{ A_a}$ and \hat{A}_b
L	Frame length bound
	Power of noise
t_i	The scheduled slot index for U_i , $t_i \in [1; L]$
$X_{ij}^{(m)}$	Bit error numbers when U_i and U_j transmit simultaneously on slot m
$P..X_a = 1 0; 0//$	The probability that the decoding symbol of U_a is 1, given both U_a and U_b transmit data bit 0 simultaneously

actually characterizes the loss of signal power as the signal propagates through the channel from a user to the sink. We assume the channel gain keeps constant during the time span of a frame, which is suitable for slow-fading channels.

When two users, Alice and Bob, transmit to the sink at the same time, the received signal Y is as followed:

$$Y = \sqrt{P_a}G_aX_a + \sqrt{P_b}G_bX_b + n_0 \quad (1)$$

where P_a and P_b are the transmitting powers of Alice and Bob. G_a and G_b are their channel gains. n_0 is the additive white Gaussian noise which obeys $N(0; \sigma^2)$, where σ^2 is the power of noise, X_a and X_b are the symbols transmitted by Alice and Bob, respectively. When Alice transmits digital data '1', X_a equals to 1, it equals to -1 otherwise.

By normalizing Y , we get

$$\bar{Y} = \frac{Y}{\sigma} = \frac{\sqrt{P_a}G_a}{\sigma}X_a + \frac{\sqrt{P_b}G_b}{\sigma}X_b + \frac{n_0}{\sigma}$$

Definition 1. For user U_a whose channel gain is G_a , its normalized received amplitude is $A_a = \frac{\sqrt{P_a}G_a}{\sigma}$ when its transmit power is P_a .

The normalized received signal \bar{Y} for Y in (1) is thus

$$\bar{Y} = A_aX_a + A_bX_b + \frac{n_0}{\sigma} \quad (2)$$

The normalized received signal \bar{Y} thus follows the Gaussian distribution whose mean is $A_aX_a + A_bX_b$ and variance is 1. Because the BPSK signal is decoded by a zero-crossing detector, the decoding results of Y and \bar{Y} are the same.

We assume that n users have data to be transmitted,¹ and the access delay of every user should be no larger than the time span of L slots, where $n \leq 2L$ must be held.

In classic communication theory, the reliability of a transmission is measured by the expected Bit Error Rate (BER) of the transmission. Therefore, for parallel transmissions, it is reasonable that the transmission reliability is defined as the mean of their expected BERs in this paper.

¹ At the beginning of a frame, these users which have transmission tasks will report themselves to the sink via control channel. Since we only need to find the users which try to be transmitters of the upcoming frame, method based on compressive sensing, can achieve the goal with low overhead [28].

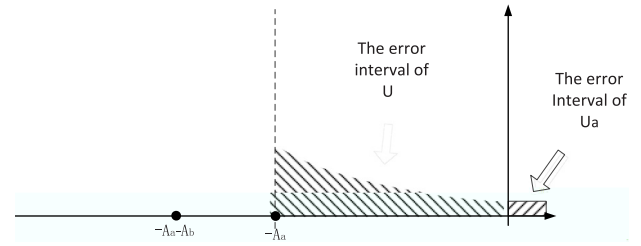


Fig. 2. The error intervals of U_a and U_b for transmitting (0, 0).

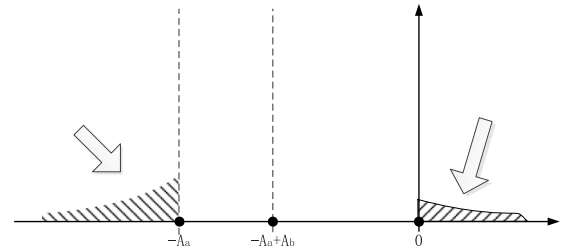


Fig. 3. The error intervals of U_a and U_b for transmitting (0, 1).

4. Preliminary and analysis of two parallel users

This section provides some preliminaries. We first present an explicit closed-form expression of BER for BPSK based 2-SIC receiver in Section 4.1. Then, we present the optimal power allocation and scheduling strategy for two parallel users in Section 4.2. Besides, some associated inferences are introduced in Sections 4.3 and 4.4. They also lay theory foundations for finding an optimal algorithm with low complexity. The optimal power allocation for two parallel users is proposed in Section 4.5.

4.1. Close-form BER expression of two parallel users

Two users, U_a and U_b , are assumed to transmit simultaneously. Besides, all symbols are assumed to have equal probability of occurrence, which is usually admitted after source coding.

The normalized received amplitude of U_a is A_a , and that of U_b is A_b , and we suppose $A_a > A_b$. According to the principle of SIC decoder, U_a will be decoded first.

When both U_a and U_b transmit data '0', as shown in Fig. 2, based on the presumption of Gaussian distribution of noise power and the principle of BPSK decoders, the decision interval for X_a to be +1 is $(0; \infty)$, and the decision interval for X_b to be +1 is $(-A_a; 0)$ if U_a decodes correctly. Therefore, the error probability of determining U_a is

$$P..X_a = 1|0; 0// = \frac{1}{\sqrt{2}} \int_{A_a+A_b}^{\infty} e^{-\frac{t^2}{2}} dt = Q..A_a + A_b/$$

, where $Q..x/$ denotes Q function which is defined as $Q..x/ = \frac{1}{\sqrt{2}} \int_x^{\infty} e^{-\frac{t^2}{2}} dt$, and $(0; \infty)$ means that both U_a and U_b simultaneously transmit data '0'.

Only when the symbol from U_a is decoded successfully, that of U_b can be correctly decoded. Therefore, the error probability of determining U_b provided U_a is decoded correctly is

Only when the symbol from U_a is decoded successfully, that of U_b can be correctly decoded. Therefore, the error probability of determining U_b provided U_a is decoded correctly is

$$P..X_b = 1|X_a = *1/^{tm}.0; 0// = \frac{\frac{1}{\sqrt{2}} \int_{A_b}^{A_a+A_b} e^{-\frac{t^2}{2}} dt}{\frac{1}{\sqrt{2}} \int_{-A_a-A_b}^{\infty} e^{-\frac{t^2}{2}} dt} = \frac{Q..A_b/ * Q..A_a + A_b/}{Q..*..A_a + A_b//}$$

$P..X_b = 1/|..X_a = *1/^{TM}.0;0//$ is the probability that symbol of U_b is decoded as 1, given that (1).symbol of U_a has been decoded as -1; (2).both U_a and U_b transmit data bit 0 simultaneously. Similarly, when both U_a and U_b transmit data '1', we get

$$P..X_a = *1/|.1;1// = P..X_a = 1/|.0;0//, \\ P..X_b = *1/|..X_a = *1/^{TM}.1;1// = P..X_b = 1/|..X_a = *1/^{TM}.0;0//.$$

The above related equations reveal some probabilities in decoding when Alice and Bob transmit same data simultaneously. Similarly, we present some probabilities in decoding when distinct data are transmitted parallel.

As shown in Fig. 3, where U_a transmits '0' and U_b transmits '1', the decision interval for X_a to be +1 is $0; \emptyset/$, and the decision interval for X_b to be *1 is $*\emptyset; *A_a/$ if U_a decodes correctly. Therefore,

$$P..X_a = 1/|.0;1// = \frac{1}{\sqrt{2}} \int_{A_a * A_b}^{\emptyset} e^{-\frac{t^2}{2}} dt = Q.A_a * A_b/;$$

$$P..X_b = *1/|..X_a = *1/^{TM}.0;1// = \frac{\frac{1}{\sqrt{2}} \int_{A_b}^{\emptyset} e^{-\frac{t^2}{2}} dt}{\frac{1}{\sqrt{2}} \int_{*A_a * A_b}^{\emptyset} e^{-\frac{t^2}{2}} dt} \\ = \frac{Q.A_b/}{Q.*.A_a * A_b//};$$

Similarly, $P..X_a = *1/|.1;0// = P..X_a = 1/|.0;1//$, and $P..X_b = 1/|..X_a = 1/^{TM}.1;0// = P..X_b = *1/|..X_a = *1/^{TM}.0;1//$.

So the expect of the error bit number $E.BE.A_a;A_b//$ is

$$E.BE.A_a;A_b// = P..X_a = 1/|.0;0// + P..X_a = 1/|.0;1// + \\ P..X_b = 1/|..X_a = 1/^{TM}.1;0// + P..X_b = 1/^{TM}.1;0// \\ P..X_b = 1/|..X_a = *1/^{TM}.0;0// + P..X_b = *1/^{TM}.0;0//$$

and thus average of the two users' BERs is

$$BER.A_a;A_b/ = \frac{1}{2} E.BE.A_a;A_b// \\ = \frac{Q.A_b/ + Q.A_a * A_b/ + \frac{1}{2} Q.A_a + A_b/}{2} \quad (3)$$

Based on the above closed-form expression, we can now present some characteristics of $BER.A_a;A_b/$.

4.2. Preliminary and minimal BER of two users in one slot

Lemma 1. $BER.A_a;A_b/$ is a decreasing function of A_a .

Proof. The lemma is obvious because

$$\frac{\partial BER.A_a;A_b/}{\partial A_a} = \frac{1}{2\sqrt{2}} * e^{-\frac{A_a + A_b/2}{2}} * \frac{1}{2} e^{-\frac{A_a + A_b/2}{2}} / < 0;$$

Lemma 1 reveals that the firstly-decoded signal should be in its maximal power for achieving minimum BER. Next, Lemma 2 shows that the optimal power of U_b is unique if the power of U_a is given.

Lemma 2. For any given value for A_a , if $A_a \geq \sqrt{5}$, there is a unique value for A_b , which is notated as $A_{|A_a}$, such that $A_{|A_a} = \arg \min_{A_b} BER.A_a;A_b/$.

Proof. The partial derivative of A_b is

$$\frac{\partial BER.A_a;A_b/}{\partial A_b} = \frac{1}{2\sqrt{2}} * e^{-\frac{A_b^2}{2}} + e^{-\frac{A_a + A_b/2}{2}} * \frac{1}{2} e^{-\frac{A_a + A_b/2}{2}} / \quad (4)$$

For a given A_a , let $f.A_b/ = \frac{\partial BER.A_a;A_b/}{\partial A_b}$. Obviously, it is a monotonically increasing function of A_b . Besides, it can be easily verified

that $f.0/ = \frac{1}{2\sqrt{2}} * 1 + \frac{1}{2} e^{-\frac{A_a^2}{2}} / < 0$, and $f.A_a/ = \frac{1}{2\sqrt{2}} * 1 * \frac{1}{2} e^{-2A_a^2} * e^{-\frac{A_a^2}{2}} / > 0$ if $A_a \geq \sqrt{5}$. Based on the well-known mean value theorem for monotonic functions, there is one and only one value $A_{|A_a}$ for A_b , where $A_{|A_a} < A_a$, such that $f.A_{|A_a}/ = 0$. In other words, when

$0 < A_b < A_{|A_a}$, $BER.A_a;A_b/$ is a decreasing function of A_b . When $A_b > A_{|A_a}$, $BER.A_a;A_b/$ is an increasing function of A_b .

Based on the above proof of Lemma 2, if $A_{|A_a}$ is achievable, $A_{|A_a}$ is obviously the theoretically optimal² received amplitude of the second-decoded user when the received amplitude of the first-decoded user is A_a . Further, we list two mathematical properties for $A_{|A_a}$, which are vital to the proof of Lemma 6 below.

Lemma 3. For given A_a , the theoretical optimal received amplitude of the second-decoded user is denoted by $A_{|A_a}$. Then, $A_{|A_a}$ is an increasing function of A_a if $A_a * A_{|A_a} > 1$.

Proof. See in Appendix A.

Lemma 4. $A_a * A_{|A_a} > 1$ for any $A_a \geq \sqrt{5}$.

Proof. See in Appendix B.

Based on the conclusions of this subsection, we have some inferences in the following two subsections, and these inferences are essential for an optimal algorithm with low complexity.

4.3. Minimal BER of three users in two slots

A note which will be frequently used in the remainder of this paper is as follows, if both U_a and U_b monopoly a slot, their average BER is denoted by $BER.A_a;A_b/$, where

$$BER.A_a;A_b/ = \frac{Q.A_a/ + Q.A_b/}{2} \quad (5)$$

Lemma 5 below reveals the reliability-optimal user pairing strategy for three users.

Lemma 5. For three users, U_a , U_b and U_c , if their normalized received amplitudes satisfy $A_a > A_b > A_c$, the following inequalities hold.³

- (1) $BER.A_a;A_c;A_b/ < BER.A_b;A_c;A_a/$,
- (2) $BER.A_a;A_c;A_b/ < BER.A_a;A_b;A_c/$.

Proof. Based on (3) and (5), $BER.A_a;A_c;A_b/ = \frac{1}{3} * Q.A_c/ + Q.A_a * A_c/ + \frac{1}{2} Q.A_a + A_c/ + Q.A_b//$, $BER.A_b;A_c;A_a/ = \frac{1}{3} * Q.A_c/ + Q.A_b * A_c/ + \frac{1}{2} Q.A_b + A_c/ + Q.A_a//$, and $BER.A_a;A_b;A_c/ = \frac{1}{3} * Q.A_b/ + Q.A_a * A_b/ + \frac{1}{2} Q.A_a + A_b/ + Q.A_c//$.

Let $g_1.t/ = \frac{1}{3} * Q.t/ * Q.t * A_b + A_a//$, therefore, $g_1.t/ = \frac{1}{3} * e^{-\frac{t^2}{2}} + e^{-\frac{t + A_a * A_b/2}{2}} / < 0$ since $A_a > A_b$.

$BER.A_b;A_c;A_a/ * BER.A_a;A_c;A_b/ = g_1.A_b * A_c/ * g_1.A_b/ + \frac{1}{2} * Q.A_b + A_c/ * Q.A_a + A_c//$. On one hand, $Q.A_b + A_c/ * Q.A_a + A_c/ > 0$ since $Q.x/$ is a decreasing function. On the other hand, $g_1.A_b * A_c/ * g_1.A_b/ > 0$ since $g_1.t/ < 0$. So, $BER.A_a;A_c;A_b/ < BER.A_b;A_c;A_a/$.

Let $g_2.t/ = \frac{1}{3} * Q.t/ * Q.t * A_c + A_b//$, therefore, $g_2.t/ = \frac{1}{3} * e^{-\frac{t^2}{2}} + e^{-\frac{t + A_a * A_c/2}{2}} / < 0$ since $A_b > A_c$. $BER.A_a;A_b;A_c/ * BER.A_a;A_c;A_b/ = \frac{g_2.A_a * A_b/ * g_2.A_a + A_c/}{2} + \frac{Q.A_a * A_b/ * Q.A_a * A_c/}{2} * g_2.A_a * A_b/ * g_2.A_a * A_c/ > 0$ since $g_2.t/ < 0$. $Q.A_a * A_b/ * Q.A_a * A_c/ > 0$ since $Q.x/$ is a decreasing function. So, $BER.A_a;A_c;A_b/ < BER.A_a;A_b;A_c/$.

² The amplitude may be infeasible if it is larger than the maximal received amplitude, and thus theoretically optimal is used.

³ $BER.A_a;A_b;A_c/$ is the average BER when U_a and U_b share a slot while U_c is monopolize another slot, and their transmit powers are $TP_a.A_a/$, $TP_b.A_b/$ and $TP_c.A_c/$, respectively, where $TP_y.x/ = \frac{x}{C_y} / 2$

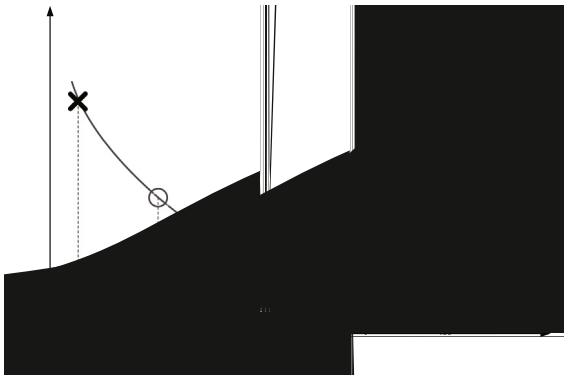


Fig. 4. Convexity of $r_1.t$.

4.4. Minimal BER of four users in two slots

Lemma 6 below reveals the reliability-optimal user pairing strategy for four users.

Lemma 6. Four users, U_a, U_b, U_c and U_d ,

(1) if their normalized received amplitudes satisfy $A_a > A_b > A_{|A_b} \geq A_c > A_d$ and $A_b > \sqrt{5}$, then $BER_{A_a; A_c; A_b; A_d} < BER_{A_a; A_d; A_b; A_c}$ holds.⁴

(2) if their normalized received amplitudes satisfy $A_a > A_b > A_c > A_d$, then $BER_{A_a; A_c; A_b; A_d} < BER_{A_a; A_b; A_c; A_d}$ holds.

Proof. $BER_{A_a; A_c; A_b; A_d} = \frac{1}{4} \cdot Q.A_d / + Q.A_b * A_d / + \frac{1}{2} Q.A_b + A_d / + Q.A_c / + Q.A_a * A_c / + \frac{1}{2} Q.A_a + A_c //$,
 $BER_{A_a; A_d; A_b; A_c} = \frac{1}{4} \cdot Q.A_d / + Q.A_a * A_d / + \frac{1}{2} Q.A_a + A_d / + Q.A_c / + Q.A_b * A_c / + \frac{1}{2} Q.A_b + A_c //$,
 $BER_{A_a; A_b; A_c; A_d} = \frac{1}{4} \cdot Q.A_b / + Q.A_a * A_b / + \frac{1}{2} Q.A_a + A_b / + Q.A_d / + Q.A_c * A_d / + \frac{1}{2} Q.A_c + A_d //$.

(1) Let $r_1.t / = \frac{1}{4} \cdot Q.t / * Q.t * A_b + A_a //$, $r_1.t /$ and $r_1.t /$ are the first-order and the second-order derivatives of $r_1.t /$, respectively, then $r_1.t / = \frac{1}{4} \cdot e^{* \frac{t^2}{2}} + e^{* \frac{t+A_a * A_b / 2}} / < 0$, and $r_1.t / = \frac{1}{4} \cdot t e^{* \frac{t^2}{2}} * t + A_a * A_b / e^{* \frac{t+A_a * A_b / 2}} /$.

Further, let $h.t / = t e^{* \frac{t^2}{2}}$, then $r_1.t / = \frac{1}{2} \cdot h.t / * h.t + A_a * A_b //$. Obviously, $h.t /$ is a decreasing function when $t \in [1; \infty /)$, and $r_1.t / > 0$ when $t \in [1; \infty /)$, i.e., $r_1.t /$ is convex in $[1; \infty /)$. Based on Lemma 4, $A_b * A_{|A_b} > 1$ since $A_b > \sqrt{5}$. Besides, since $A_{|A_b} > A_c$ based on the prerequisite of Lemma 6, $A_b * A_c \geq 1$. So, $r_1.t /$ is convex for $t \in [A_b * A_c; \infty /)$.

$BER_{A_a; A_d; A_b; A_c} * BER_{A_a; A_c; A_b; A_d} / = r_1.A_b * A_c / * r_1.A_b * A_d / * \frac{1}{2} r_1.A_b + A_d / + \frac{1}{2} r_1.A_b + A_c / = \frac{r_1.A_b * A_c / * r_1.A_b * A_d /}{2} + \frac{r_1.A_b * A_c / + r_1.A_b + A_c / * r_1.A_b * A_d / * r_1.A_b + A_d /}{2}$. We judge its sign as follows, on one hand, $r_1.A_b * A_c / * r_1.A_b * A_d / > 0$ since $r_1.t / < 0$ for any t . On the other hand, just as shown by Fig. 4, since $r_1.t /$ is convex for $t \in [A_b * A_c; \infty /)$, $r_1.A_b * A_c / + r_1.A_b + A_c / > r_1.A_b * A_d / + r_1.A_b + A_d /$. Thus, $BER_{A_a; A_c; A_b; A_d} < BER_{A_a; A_d; A_b; A_c}$.

(2) Let $r_2.t / = \frac{1}{4} \cdot Q.t / * Q.t * A_c + A_b //$, therefore, $r_2.t / = e^{* \frac{t^2}{2}} + e^{* \frac{t+A_b * A_c / 2}} < 0$.

$BER_{A_a; A_b; A_c; A_d} * BER_{A_a; A_c; A_b; A_d} / = r_2.A_c * A_d / * r_2.A_c / + r_2.A_a * A_b / + \frac{1}{2} \cdot r_2.A_c + A_d / * r_2.A_a + A_c //$.

$r_2.A_c * A_d / * r_2.A_c / > 0$, and $r_2.A_c + A_d / > r_2.A_a + A_c / > 0$, since $r_2.t / < 0$.

Thus, $BER_{A_a; A_c; A_b; A_d} < BER_{A_a; A_b; A_c; A_d}$.

⁴ $BER_{A_a; A_b; A_c; A_d} /$ is the average BER when U_a and U_b share a slot, while U_c and U_d share another slot, and their received amplitudes are A_a, A_b, A_c and A_d , respectively.

4.5. Optimal power allocation for two parallel users

Based on the above results of the closed-form BER expression (3), the optimal power allocation strategy for two parallel users is derived in the following subsection. Note that $TP_{y,x} / = \frac{x}{G_y} / 2$, which computes the transmitting power of U_y if its received amplitude at the sink is x .

Lemma 7. Assume that the maximal normalized received amplitudes of two parallel users U_a and U_b are \hat{A}_a and \hat{A}_b , respectively. If U_a is decoded firstly, the minimal BER is achieved only when U_a transmits with its maximal power $TP_a.A_{|A_a} /$, and the transmit power of U_b is $TP_b.min^A_{|A_a}; \hat{A}_b /$ at the same time.

Proof. The proof can be got directly based on Lemmas 1 and 2 as follows. According to Lemma 1, the firstly-decoded signal should be transmitted in its maximal power for achieving minimum BER. According to Lemma 2, the optimum is achieved when U_b transmits with power $TP_b.A_{|A_a} /$ if $A_{|A_a} \leq \hat{A}_b$. On the contrary, if $A_{|A_a} > \hat{A}_b$, U_b should transmit using its maximal power, i.e., $TP_b.\hat{A}_b /$.

In the remainder of this paper, $min^A_{|A_a}; \hat{A}_b /$ is denoted by $\hat{A}_{b|A_a}$ for short.

Based on Lemma 7, the theoretically minimum BER is $BER_{\hat{A}_a; \hat{A}_{b|A_a} /} = \frac{1}{2} \cdot Q.\hat{A}_{b|A_a} / + Q.\hat{A}_a * \hat{A}_{b|A_a} / + \frac{1}{2} Q.\hat{A}_a + \hat{A}_{b|A_a} //$.

Lemma 7 is for determining the optimal transmit powers of two parallel users, given their decoding order. The next lemma reveals the best decoding order for two parallel users.

Lemma 8. For two parallel users U_a and U_b with their channel gains being G_a and G_b , respectively, if they have the same transmit power bound P_{max} and $G_a > G_b$. The minimum BER can be achieved only when U_a is decoded firstly.

Proof. Since U_a and U_b have the same maximal transmit power and $G_a > G_b$, we have $\hat{A}_b < \hat{A}_a$.

If U_b is decoded firstly, according to Lemma 4, the minimum BER is $BER_{\hat{A}_b; \hat{A}_{a|A_b} /}$.

Otherwise, if U_a is decoded firstly,

(1) if $\hat{A}_b > A_{|A_a}$, the optimal BER is thus $BER_{\hat{A}_a; A_{|A_a} /}$ based on Lemma 7. Based on Lemma 1, $BER_{\hat{A}_b; \hat{A}_{a|A_b} /} > BER_{\hat{A}_a; \hat{A}_{a|A_b} /}$. Note that $A_{|A_b} = \hat{A}_{a|A_b}$ if $\hat{A}_b > A_{|A_a}$. Therefore, $BER_{\hat{A}_b; \hat{A}_{a|A_b} /} > BER_{\hat{A}_a; A_{|A_a} /}$.

(2) if $\hat{A}_b \leq A_{|A_a}$, the optimal BER is thus $BER_{\hat{A}_a; \hat{A}_b /}$ based on Lemma 7. Based on Lemma 1, $BER_{\hat{A}_b; \hat{A}_{a|A_b} /} > BER_{\hat{A}_a; \hat{A}_{a|A_b} /}$. Based on Lemma 2, $BER_{\hat{A}_a; A_{|A_b} /} \geq BER_{\hat{A}_a; \hat{A}_b /}$ if $\hat{A}_b \leq A_{|A_a}$. Thus, $BER_{\hat{A}_b; \hat{A}_{a|A_b} /} > BER_{\hat{A}_a; \hat{A}_b /}$.

In conclusion, the minimum BER can be achieved only when U_a is decoded firstly.

5. Problem formulation and solving

In this section, The problem of reliable uplink scheduling with guaranteed real-time performance for N Users is formulated. To solve it, Lemma 9 reveals that all provided slots should be utilized, which is the foundation. In Theorems 1 and 2, the optimal scheduling strategies for three and four users with two time slots are given, respectively. Then the general case, i.e., the scenario of N users in L time slots, is solved by Algorithm 1. and its optimum is proven by Theorem 3.

5.1. Problem formulation

Definition 2. Reliable Uplink Scheduling for 2-SIC (RUS-2SIC). We are given a single-hop network consisting of a sink equipped with a perfect BPSK-based 2-SIC receiver and n users $U_1; U_2; \dots; U_n$ whose channel gains are $G_1; G_2; \dots; G_n$, respectively. Without loss of generality

(W.l.o.g.), we assume $G_1 \geq G_2 \geq \dots \geq G_n$, the maximal transmit powers of users are same, and noise power is n_0 for all users. Denote their transmit powers to be $p_1; p_2; \dots; p_n$, respectively. Assign transmit powers to and schedule the n users such that the average BER of the n users is minimized under the following constraints: (1) Every user is scheduled only once in a frame. (2) The frame length is no larger than the given value L .

The RUS-2SIC can be formulated as follows.

$$\min_{\substack{\hat{t}_1; \hat{t}_2; \dots; \hat{t}_n; \\ p_1; p_2; \dots; p_n}} \frac{1}{n} \sum_{m=1}^L \sum_{\substack{i \in [1; n] \\ j \in [1; n]}} x_{ij}^{(m)} \quad (6a)$$

$$x_{ij}^{(m)} = \begin{cases} BE(A_i; A_j) & .t_i = t_j = m/ \\ BE(A_i) & .t_i = m/\text{and}.t_j \neq m/ \\ BE(A_j) & .t_j = m/\text{and}.t_i \neq m/ \\ 0 & .t_j \neq m/\text{and}.t_i \neq m/ \end{cases} \quad (6b)$$

$$\text{s.t: } 0 \leq \sum_{i=1}^n 1.t_i = j/ \leq 2 \quad \hat{A}_j \in [1; L] \quad (6c)$$

$$t_i \in [1; S]; \quad \hat{A}_i \in [1; n] \quad (6d)$$

$$A_i = \frac{\sqrt{p_i} G_i}{\hat{A}_i} \quad \hat{A}_i \in [1; n]; \quad (6e)$$

where t_i is the scheduling slot index for U_i , $1./$ is the indication function. Obviously, the system reliability is influenced by both $\hat{t}_1; \hat{t}_2; \dots; \hat{t}_n$ and $p_1; p_2; \dots; p_n$. L is the frame length bound, which is for gauging the real-time performance.⁵

5.2. Problem solving

It seems that RUS-2SIC is a joint optimization problem, and thus high time complexity will be inevitable if it is solved by the optimization-based algorithms. We, however, propose a low-complexity algorithm. To clearly explain the idea of the algorithm, we present two key attributes of the optimal user pairing strategy, i.e., [Theorems 2](#) and [3](#). Then we propose an optimal scheduling strategy based on the two key attributes, and prove its uniqueness.

Lemma 9. *If $L \leq n \leq 2L$, for the optimal solution to RUS-2SIC, there is no idle slot.*

Proof. See in [Appendix C](#).

Lemma 9 is vital although intuitive, and it is the foundation of the optimal strategy. The next two theorems reveal the optimal user pairing strategy between any two slots, and the two theorems are a key criterion for the optimal user pairing strategy of RUS-2SIC.

Theorem 1. *For three users $U_1; U_2; U_3$, whose maximum normalized received amplitudes satisfy $\hat{A}_1 > \hat{A}_2 > \hat{A}_3$, if they are assigned to two slots, the optimal user pairing will be $\{U_1; U_3\}; \{U_2\}$, i.e., U_1 shares a slot with U_3 , and U_2 monopolizes the other one.*

Proof. There are obviously three pairing candidates: $\{U_1; U_3\}; \{U_2\}$, $\{U_2; U_3\}; \{U_1\}$ and $\{U_1; U_2\}; \{U_3\}$. By comparing their optimal BERs directly, $\{U_1; U_3\}; \{U_2\}$ can be proven to be optimal as follows.

Due to [Lemma 5](#), [Lemmas 7](#) and [8](#), the optimal amplitude assignment for $\{U_1; U_3\}; \{U_2\}$ is $\{\hat{A}_1; \hat{A}_3\}; \hat{A}_2$, and these for $\{U_1; U_2\}; \{U_3\}$ and $\{U_2; U_3\}; \{U_1\}$ are $\{\hat{A}_1; \hat{A}_2\}; \hat{A}_3$ and $\{\hat{A}_2; \hat{A}_3\}; \hat{A}_1$, respectively.

(1) Comparing the optimal BER of $\{U_1; U_3\}; \{U_2\}$ with that of $\{U_1; U_2\}; \{U_3\}$. Since $\hat{A}_1 > \hat{A}_2 > \hat{A}_3$, due to [Lemma 5](#), $BER(\hat{A}_2; \hat{A}_3; \hat{A}_1) > BER(\hat{A}_1; \hat{A}_3; \hat{A}_2)$. Due to the optimum revealed by [Lemma 7](#),

$BER(\hat{A}_1; \hat{A}_3; \hat{A}_2) \geq BER(\hat{A}_1; \hat{A}_3; \hat{A}_1)$. Thus, as to the reliability, $\{U_1; U_3\}; \{U_2\}$ is better than $\{U_1; U_2\}; \{U_3\}$.

(2) Comparing the optimal BER of $\{U_1; U_3\}; \{U_2\}$ with that of $\{U_2; U_3\}; \{U_1\}$.

If $\hat{A}_1 \geq \hat{A}_3$, the optimal amplitude assignment for $\{U_1; U_3\}; \{U_2\}$ is $\{\hat{A}_1; \hat{A}_3\}; \hat{A}_2$. Due to [Lemma 5](#), $BER(\hat{A}_1; \hat{A}_3; \hat{A}_2) > BER(\hat{A}_1; \hat{A}_3; \hat{A}_1)$ since $\hat{A}_1 > \hat{A}_2 > \hat{A}_3$. Due to [Lemma 1](#), $BER(\hat{A}_1; \hat{A}_3; \hat{A}_2) \geq BER(\hat{A}_1; \hat{A}_3; \hat{A}_1)$ since $\hat{A}_2 \leq \hat{A}_1$. Thus, $BER(\hat{A}_1; \hat{A}_3; \hat{A}_2) >$

⁵ To achieve the guaranteed real-time performance, the time span of a frame must be no greater than half of the transmission delay bound in typical settings. Their relationship will be revealed in detail in [Section 6](#).

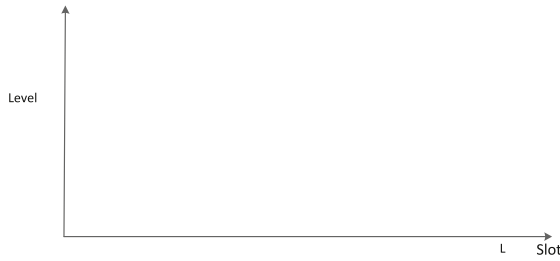


Fig. 5. Optimal user pairing strategy.

is L where $L \in \{n/2; n\}$. Otherwise, any other pairing strategy must be contradicted with either [Theorems 2](#) or [3](#).

To describe the above example formally, the reliability-optimal low-complexity algorithm for RUS-2SIC as follows.

Algorithm 1. An optimal algorithm for RUS-2SIC {
 Input: N : users set; $CG[n]$: channel gains of users to the sink; σ^2 : noise power; P_{\max} : maximum transmission power; L : guaranteed delay; \hat{A} : max received amplitude of each user
 Output: $GM[L]$: optimal user pairing method; PA : optimal power allocation
 1. sort N users in descending order of their channel gains to the sink, and w.l.o.g., assume $CG[i] \geq CG[i+1], i = 1; 2; \dots; n * 1/2$; 2. $GM = \emptyset$;
 3. for $i = 1; i \leq n; i++$ $\hat{A}[i] = \frac{\sqrt{P_{\max}} * CG[i]}{n_0}$; //compute the maximal normalized received amplitude of each user
 4. for $j = 1; j \leq L; j++$ { //designate the optimal strategy
 5. if $j \leq n * L/2$ $GM[j] = \langle U_j; U_{j+L} \rangle$;
 else $GM[j] = \hat{U}_j$;
 6. for $j = 1; j \leq L; j++$ { //assign transmitting powers
 7. if $j \leq n * L/2$
 $PA[j] = P_{\max}; PA[j+L] = \hat{A}^2 P_{\max} \cdot \min(\hat{A}_{|A[j]|}, \hat{A}_{|A[j+L]|})^2$; //The power allocation of User j and User $j+L$ in the j th slot
 8. else $PA[j] = P_{\max}$;

We have a simple explanation for Algorithm 1 as follows. We first sort all users by their channel gains to the sink, then we calculate their maximum received amplitudes possible. Just as that illustrated in [Fig. 5](#), line 4 and line 5 directly designate the optimal user pairing slot by slot. In line 5, $\langle U_j; U_{j+L} \rangle$ implies that U_j and U_{j+L} share a slot, and U_j will be decoded firstly,⁶ and \hat{U}_j implies that U_j monopolies a slot.⁷ From line 6 to line 8, we assign transmitting power for every user, where $\hat{A}^2 P_{\max} \cdot \min(\hat{A}_{|A[j]|}, \hat{A}_{|A[j+L]|})^2$ is to compute the transmit power if its normalized received amplitude is A , and $\hat{A}_{|A[j]|}$ is the theoretical optimal normalized received amplitude of U_{j+L} since U_j and U_{j+L} share a slot and U_j is decoded firstly.

Theorem 3. Algorithm 1 outputs an optimal solution to RUS-2SIC.

Proof. We prove it by contradictions. If there is another strategy differing from that output by Algorithm 1, there must be two user pairings, which occupy two slots and disobey the necessary condition for the optimality. Specifically, if both of them are full slots, then it disobeys [Theorem 2](#). If one is a full slot and the other is a half-full slot, then it disobeys [Theorem 1](#). In all, we cannot find a better user pairings strategy than that output by Algorithm 1.

A prominent merit of Algorithm 1 is its low complexity of $\mathcal{O}(n \log n / \log)$, which is mainly caused by the sorting algorithm at line 1.

⁶ We use $\langle U_j; U_i \rangle$ instead of $\hat{U}_j; U_i$ to intentionally show the decoding order of U_i and U_j here and hereafter.

⁷ For convenience, the monopolized slot is termed as half-full slot, while the shared case is termed as full slot.

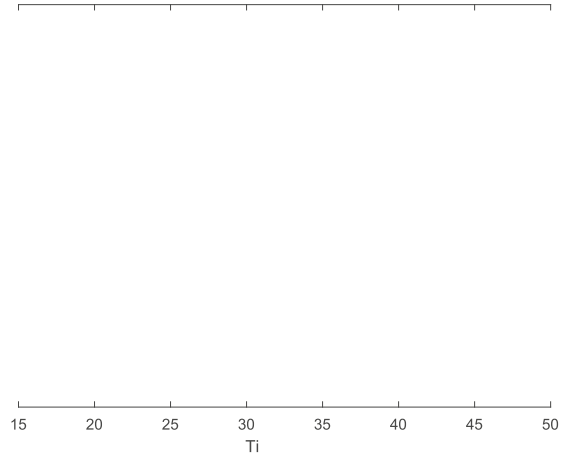


Fig. 6. Average BER with users and delay bounds.

6. Performance evaluations

We evaluate the relationship between the transmission reliability and the delay bound by simulations in the first step. [Fig. 6](#) illustrates the relationship among the average BER, the delay bound and the user number. Some simulation parameters are as follows: all users are deployed randomly in a ring area with the internal radius and the external radius to be 500m and 1200m respectively, and a sink is located at the center of the ring. The noise power is -126 dBm, which the power spectral density is -173 dBm/Hz, while the bandwidth is 50 kHz. The maximum transmitting power is 16 dBm for all users. The channel gain model is $CG = 20 \log(f) + 26 \log(d) + 19.2$ where CG is the channel gain, d is the distance to the sink, and f is 5 GHz.

How to set the parameter of the real-time performance, i.e., L in formula (9), is vital for delay guarantee. Using the time span of a slot as the basic time unit, we assume that the data collection cycles of all users are the same, which are denoted by T_s . The maximal delay bound is assumed to be T_b , which is the real-time performance bound. Obviously, only if $2L \leq T_b \leq T_s$ holds, the real-time performance of every user will be guaranteed. Therefore, $\lfloor T_b/2 \rfloor$ is the maximal value for L to guarantee the delay performance. Further, if $n \leq 2L$, every user will be given a transmitting opportunity in a frame. Therefore, the real-time performance is always guaranteed.

In [Fig. 6](#), we can find that for a given user number, the average BER decreases exponentially with the increase of delay bound. In other words, the transmission reliability is greatly influenced by the real-time performance requirements. The reason is as follows. Given more relaxed real-time performance, more half-full slots will come into being in the optimal strategy generated by Algorithm 1. Since the average BER of a half-full slot is in general far less than that of a full slot, the transmission reliability thus increases. With the same delay bound requirement, the average BER always increases with the increment of the user number. The reason is also due to the fact that the increase of user number results in less half-full slots. Besides, we note that there is a sharp knee point at the end of each curve in [Fig. 6](#). Indeed, it is virtually the orthogonal multiple access transmissions, where every user monopolies one slot.

Using the same simulation parameters, we compare the running time of Algorithm 1 with that using the Edmond's blossom method. On our personal computer with i7-4710HQ CPU and 16GB memory, their running times are illustrated in [Fig. 7](#). Obviously, both of them grow rapidly with the user number. For any given parameter, the running time of Algorithm 1 is less by three orders of magnitude of that utilizing the Edmond's blossom method. The reason is obvious because the complexity of Algorithm 1 is only $\mathcal{O}(n \log n)$, while that utilizes the Edmond's blossom method is $\mathcal{O}(n^4)$.

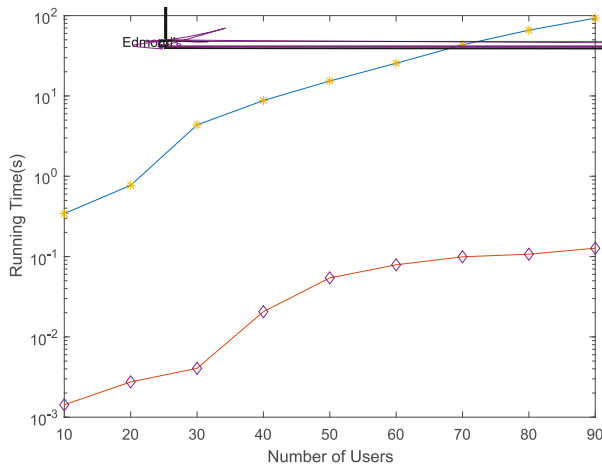


Fig. 7. Comparison of algorithms' running time.

7. Conclusions

In this paper, we analyze the transmission reliability with guaranteed real-time performance for NOMA-based uplink IWNs. We formulate the problem and present an optimal algorithm. The complexity of algorithm 1 after sorting is actually $O(n)$. The lowest complexity of sorting is quicksort whose complexity is $O(n \log n)$. So, the overall complexity is $O(n \log n)$ including the sorting process. The Both theoretical proofs and performance evaluations validate the optimality of the algorithm proposed.

Transmission reliability is a vital metric for IWNs because reliabilities are always rigidly required in industrial applications. Since power-domain NOMA is now a powerful candidate media access technique for the next-generation IWNs, finding rapid algorithms for high-reliability communications are indispensable. Our research results lay a theoretical foundation for high-reliability low-latency transmissions for the next-generation IWNs.

CRedit authorship contribution statement

Chaonong Xu: Conceptualization, Methodology, Writing - review & editing. Jianxiong Wu: Formal analysis, Software. Chao Li: Resources, Visualization.

Declaration of competing interest

The authors declare that they have no known competing financial interests or personal relationships that could have appeared to influence the work reported in this paper.

Acknowledgments

This publication is supported by National Natural Science Foundation of China under Grant 61702487.

Appendix A. The proof of Lemma 3

Based on (4), for A_a and $A_{|A_a}$, we have

$$*e^{\frac{A_a^2}{2}} + e^{\frac{A_a^2 A_{|A_a}^2}{2}} * \frac{1}{2} e^{\frac{A_a + A_{|A_a}}{2}} = 0; \tag{7}$$

In other words, A_a can be seen as a function of $A_{|A_a}$. Therefore, $\frac{\partial A_a}{\partial A_{|A_a}} =$

$$\frac{A_{|A_a} e^{\frac{A_a^2}{2}} + A_a * A_{|A_a} / e^{\frac{A_a^2 A_{|A_a}^2}{2}}}{A_a * A_{|A_a} / e^{\frac{A_a^2 A_{|A_a}^2}{2}} * \frac{1}{2} * A_{|A_a} + A_a / e^{\frac{A_a + A_{|A_a}}{2}}} + \frac{\frac{1}{2} * A_{|a} + A_a / e^{\frac{A_{|A_a} + A_a}{2}}}{A_a * A_{|A_a} / e^{\frac{A_a^2 A_{|A_a}^2}{2}} * \frac{1}{2} * A_{|A_a} + A_a / e^{\frac{A_a + A_{|A_a}}{2}}}$$

Next, we aim to reveal that $A_{|A_a}$ always increases with A_a , i.e., $\frac{\partial A_a}{\partial A_{|A_a}} > 0$. Since the numerator of (8) is larger than 0 because $A_a > A_{|A_a}$, the sign of $\frac{\partial A_a}{\partial A_{|A_a}}$ totally depends on that of its denominator of (8).

Let $g.t/ = t e^{\frac{t^2}{2}}$; $t \in (0; \infty)$. Obviously, $g'.t/ = e^{\frac{t^2}{2}} * t^2 e^{\frac{t^2}{2}}$. Thus $g.t/$ increases with $t \in (0; \infty)$, and decreases with $t \in [1; \infty)$. Now the denominator of (8) can be rewritten as $g.A_a * A_{|A_a} / * \frac{1}{2} g.A_a + A_{|A_a} /$. So, as long as $A_a * A_{|A_a} / \in (1; \infty)$, $A_a + A_{|A_a} > 1$, and thus $2g.A_a * A_{|A_a} / * g.A_a + A_{|A_a} / > g.A_a * A_{|A_a} / > 0$ because $A_a > A_{|A_a}$. In other words, $A_{|A_a}$ is an increasing function of A_a if $A_a * A_{|A_a} > 1$.

Appendix B. The proof of Lemma 4

We prove it by contradictions. Assume that $A_a * A_{|A_a} \leq 1$. According to (7),

$$e^{\frac{A_a^2 A_{|A_a}^2}{2}} = e^{\frac{A_{|A_a}^2}{2}} + \frac{1}{2} e^{\frac{A_a + A_{|A_a}}{2}}; \tag{9}$$

Since $A_a > \sqrt{5}$, the left part of (9) is thus $e^{\frac{A_a^2 A_{|A_a}^2}{2}} \geq e^{\frac{1}{2}} = 0.6065$, while the right part is thus $e^{\frac{A_{|A_a}^2}{2}} + \frac{1}{2} e^{\frac{A_a + A_{|A_a}}{2}} \leq e^{\frac{\sqrt{5} + 1}{2}} + \frac{1}{2} e^{\frac{2\sqrt{5} + 1}{2}} = 0.4671$. So it brings contradiction to (9).

A_a , the normalized received amplitude of a signal, is in fact the square root of the signal noise ratio of the first-decoded signal at the receiver side. Although $A_a > \sqrt{5}$ is required for this paper, the condition is generally true in practice.⁸

Appendix C. The proof of Lemma 9

If there is an idle slot, there is at least one slot which includes two users. W.l.o.g., assume the two users are U_i and U_j , and $G_i > G_j$. Thus, their maximal normalized received amplitudes satisfy $\hat{A}_i > \hat{A}_j$.

According to Lemmas 7 and 8, for the two parallel users, their average optimal BER is $BER.\hat{A}_i; \hat{A}_j / |A_i| = \frac{1}{2} * Q.\hat{A}_j / |A_i| + Q.\hat{A}_i * \hat{A}_j / |A_i| + \frac{1}{2} Q.\hat{A}_i + \hat{A}_j / |A_i| //$.

However, if U_i and U_j monopoly a slot respectively, the optimal average BER of them is $\frac{1}{2} * Q.\hat{A}_j / + Q.\hat{A}_i //$. Since $Q.x/$ is a decreasing function of x and $\hat{A}_j / |A_i| < \hat{A}_i$, $BER.\hat{A}_i; \hat{A}_j / |A_i| > \frac{1}{2} * Q.\hat{A}_j / + Q.\hat{A}_i //$. In other words, a smaller average BER can be got, which contradicts the assumption of the optimality.

In conclusion, there is no idle slot for the optimal solution to RUS-2SIC.

References

- [1] X. Li, D. Li, J. Wan, A.V. Vasilakos, C.-F. Lai, S. Wang, A review of industrial wireless networks in the context of industry 4.0. *Wirel. Netw.* 23 (2017) 23–41, <http://dx.doi.org/10.1007/s11276-015-1133-7>.
- [2] C. Xu, H. Ding, Y.-J. Xu, Low-complexity uplink scheduling algorithms with power control in successive interference cancellation based wireless multiuser systems, *Wirel. Netw.* 25 (1) (2017) 321–334, <http://dx.doi.org/10.1007/s11276-017-1561-7>.

⁸ If A_a is $\sqrt{5}$, $A_{|A_a}$ is 1.12, which is very near to Shannon limit.

- [3] Y. Liu, Z. Qin, M. Elkashlan, Z. Ding, A. Nallanathan, L. Hanzo, Non-orthogonal multiple access for 5G and beyond, *Proc. IEEE* 105 (12) (2017) 2347–2381, <http://dx.doi.org/10.1109/JPROC.2017.2768666>.
- [4] Y. Yu, S. Huang, J. Wang, J. Ou, Design of wireless logging instrument system for monitoring oil drilling platform, *IEEE Sens. J.* 15 (6) (2015) 3453–3458, <http://dx.doi.org/10.1109/JSEN.2015.2391280>.
- [5] B. Di, L. Song, Y. Li, G.Y. Li, Non-orthogonal multiple access for high-reliable and low-latency V2X communications in 5G systems, *IEEE J. Sel. Areas Commun.* 35 (10) (2017) 2383–2397, <http://dx.doi.org/10.1109/JSAC.2017.2726018>.
- [6] Z. Ding, X. Lei, G.K. Karagiannidis, R. Schober, J. Yuan, V.K. Bhargava, A survey on non-orthogonal multiple access for 5G networks: Research challenges and future trends, *IEEE J. Sel. Areas Commun.* 35 (10) (2017) 2181–2195, <http://dx.doi.org/10.1109/JSAC.2017.2725519>.
- [7] D. Halperin, T.E. Anderson, D. Wetherall, Taking the sting out of Carrier sense: Interference Cancellation for wireless LANs, in: *Proceedings of the 14th ACM International Conference on Mobile Computing and Networking*, ACM, New York, USA, 2008, pp. 339–350, <http://dx.doi.org/10.1145/1409944.1409983>.
- [8] T.J. Pierson, T. Peters, R. Peterson, D. Kotz, Proximity detection with single-antenna IoT devices, in: *Proceedings of the 25th Annual International Conference on Mobile Computing and Networking*, ACM, Los Cabos, Mexico, 2019, pp. 1–15, <http://dx.doi.org/10.1145/3241539.3267751>.
- [9] E. Karipidis, D. Yuan, Q. He, E.G. Larsson, Max-min power control in wireless networks with successive interference Cancellation, *IEEE Trans. Wireless Commun.* 14 (11) (2015) 6269–6282, <http://dx.doi.org/10.1109/TWC.2015.2451653>.
- [10] S. Loyka, F. Gagnon, Performance analysis of the V-BLAST algorithm: an analytical approach, *IEEE Trans. Wireless Commun.* 3 (4) (2004) 1326–1337, <http://dx.doi.org/10.1109/TWC.2004.830853>.
- [11] C. Shen, Y. Zhu, S. Zhou, J. Jiang, On the performance of V-BLAST with zero-forcing successive interference cancellation receiver, in: *IEEE Global Telecommunications Conference 2004*, Vol. 5, Dallas, TX, USA, 2004, pp. 2818–2822, <http://dx.doi.org/10.1109/GLOCOM.2004.1378868>.
- [12] M.-S.V.N. Dinh-Thuan Do, Device-to-device transmission modes in NOMA network with and without Wireless Power Transfer, *Comput. Commun.* 139 (2019) 67–77, <http://dx.doi.org/10.1016/j.comcom.2019.04.003>.
- [13] M.F. Kader, M.B. Shahab, S.Y. Shin, Non-orthogonal multiple access for a full-duplex cooperative network with virtually paired users, *Comput. Commun.* 120 (2018) 1–9, <http://dx.doi.org/10.1016/j.comcom.2018.02.010>.
- [14] X. Wang, F. Labeau, L. Mei, Closed-form BER expressions of QPSK constellation for uplink non-orthogonal multiple access, *IEEE Commun. Lett.* 21 (10) (2017) 2242–2245, <http://dx.doi.org/10.1109/LCOMM.2017.2720583>.
- [15] S. Shi, L. Yang, H. Zhu, Outage balancing in downlink nonorthogonal multiple access with statistical channel state information, *IEEE Trans. Wireless Commun.* 15 (7) (2016) 4718–4731, <http://dx.doi.org/10.1109/TWC.2016.2544922>.
- [16] C. Xu, K. Ma, Y. Xu, Y. Xu, Y. Fang, Optimal power scheduling for uplink transmissions in SIC-based industrial wireless networks with guaranteed real-time performance, *IEEE Trans. Veh. Technol.* 67 (4) (2018) 3216–3228, <http://dx.doi.org/10.1109/TVT.2017.2779784>.
- [17] H. Tabassum, E. Hossain, J. Hossain, Modeling and analysis of uplink non-orthogonal multiple access in large-scale cellular networks using Poisson cluster processes, *IEEE Trans. Commun.* 65 (8) (2017) 3555–3570, <http://dx.doi.org/10.1109/TCOMM.2017.2699180>.
- [18] H. Tabassum, E. Hossain, J. Hossain, Modeling and analysis of uplink non-orthogonal multiple access in large-scale cellular networks using Poisson cluster processes, *IEEE Trans. Commun.* 65 (8) (2017) 3555–3570, <http://dx.doi.org/10.1109/TCOMM.2017.2699180>.
- [19] T. Assaf, A. Al-Dweik, M.E. Moursi, H. Zeineldin, Exact BER performance analysis for downlink NOMA systems over nakagami- m fading channels, *IEEE Access* 7 (2019) 134539–134555, <http://dx.doi.org/10.1109/ACCESS.2019.2942113>.
- [20] F. Kara, H. Kaya, BER performances of downlink and uplink NOMA in the presence of SIC errors over fading channels, *IET Commun.* 12 (15) (2018) 1834–1844, <http://dx.doi.org/10.1049/iet-com.2018.5278>.
- [21] B. Xia, J. Wang, K. Xiao, Y. Gao, Y. Yao, S. Ma, Outage performance analysis for the advanced SIC receiver in wireless NOMA systems, *IEEE Trans. Veh. Technol.* 67 (7) (2018) 6711–6715, <http://dx.doi.org/10.1109/TVT.2018.2813524>.
- [22] G. Im, J.H. Lee, Outage probability for cooperative NOMA systems with imperfect SIC in cognitive radio networks, *IEEE Commun. Lett.* 23 (4) (2019) 692–695, <http://dx.doi.org/10.1109/LCOMM.2019.2903040>.
- [23] W. Saetan, S. Thipchaksurat, Power Allocation for Sum Rate Maximization in 5G NOMA System with Imperfect SIC: A Deep Learning Approach, in: *4th International Conference on Information Technology, InCIT*, Bangkok, Thailand, Thailand, 2019, pp. 195–198, <http://dx.doi.org/10.1109/INCIT.2019.8911864>.
- [24] A. Han, T. Lv, X. Zhang, Outage Performance of NOMA-based UAV-Assisted Communication with Imperfect SIC, in: *IEEE Wireless Communications and Networking Conference 2019*, Marrakesh, Morocco, Morocco, 2019, pp. 1–6, <http://dx.doi.org/10.1109/WCNC.2019.8885725>.
- [25] X. Liu, X. Xie, S. Wang, J. Liu, D. Yao, J. Cao, K. Li, Efficient range queries for large-scale sensor-augmented RFID systems, *IEEE/ACM Trans. Netw.* 27 (5) (2019) 1873–1886, <http://dx.doi.org/10.1109/TNET.2019.2936977>.
- [26] X. Liu, S. Chen, J. Liu, W. Qu, F. Xiao, A.X. Liu, J. Cao, J. Liu, Fast and accurate detection of unknown tags for RFID systems - hash collisions are desirable, *IEEE/ACM Trans. Netw.* 28 (1) (2020) 126–139, <http://dx.doi.org/10.1109/TNET.2019.2957239>.
- [27] D. Tweed, T. Le-Ngoc, Dynamic Resource Allocation for Uplink MIMO NOMA VWN with Imperfect SIC, in: *IEEE International Conference on Com ([.])TonCo1 RG 0 -8.5 1* W-496(T.)-81(Wcomlosed-ve50412((for0 Rrformaniu)-1(,)-587(Fast)-587(and)]TJ0 0 0 rg 0 0 2242 2245, <http://dx.doi.org/10.1109/TVT.2018.2813524>.

